American Mineralogist, Volume 76, pages 1101–1109, 1991

Single crystal Raman spectra of forsterite, fayalite, and monticellite

A. CHOPELAS
Max Planck Institut für Chemie, Postfach 3060, 6500 Mainz, Germany

ABSTRACT

Polarized single crystal Raman spectra of the fundamental modes of forsterite (Mg_2SiO_4), olivine ($Mg_{0.88}Fe_{0.12}$), fayalite (Fe_2SiO_4), and monticellite ($CaMgSiO_4$) are presented. Seven low energy modes (<450 cm^{-1}) in forsterite differ from those of all previous studies. All modes predicted by symmetry for forsterite and monticellite were observed; 34 out of 36 modes were observed for fayalite. Assignment of the modes was determined by systematics in frequency changes resulting from cation substitution. Although the lattice modes are generally mixed, likely mode assignments are made using the following observations. The lowest energy modes are assigned to SiO_4 translations and appear to be mixed with the cation translations. The lattice modes between 330 and 435 cm^{-1} in forsterite that changed the least with composition were assigned as SiO_4 rotations. The modes from 300 to 390 cm^{-1} that showed the greatest variation with composition or showed signs of two-mode behavior in the olivine Mg_{88} were assigned as M2 translations. The SiO_4 internal stretching and bending modes were assigned to the highest frequencies; they vary little from forsterite to monticellite to fayalite and appear to depend more on cation mass than volume. These assignments are consistent with previous single-crystal infrared studies of forsterite and fayalite and with mode Grüneisen parameters γ_i measured vs. pressure in that the highest γ_i values should be associated with the M2 cations and the lowest with the SiO_4 internal modes.

INTRODUCTION

The vibrational modes of olivines, important geophysical and cosmochemical phases, have been studied extensively by Raman spectroscopy (Iishi, 1978; Servoin and Piriou, 1973; Piriou and McMillan, 1983; Stidham et al., 1976; Hohler and Funck, 1973; Chopelas, 1990), infrared spectroscopy (Hofmeister, 1987; Tarte, 1963; Paques-Ledent and Tarte, 1973; Kovach et al., 1975; Hofmeister et al., 1989; plus some references given above for Raman spectroscopy), inelastic neutron scattering (Rao et al., 1988), and lattice dynamical calculations (Price et al., 1987a, 1987b). Study of these properties yields insight into the interatomic forces within the crystal structure and a basis for understanding the effect of cation substitutions on the thermodynamic properties. For example, the heat capacity and entropy can be estimated to better than 5% over a moderate temperature range (~500 K, Kieffer, 1979) from the mode frequency information obtained by infrared and Raman spectroscopy. The accuracy in estimating these quantities can increase to better than 0.5% over a larger temperature range (>1000 K) if all of the infrared and Raman modes are enumerated and assigned to atomic motions. The detailed mode assignments provide an accurate method for estimating the frequencies of inactive or unobserved modes, thereby yielding more precise information on the frequency distribution or density of states (see Hofmeister, 1987; Hofmeister and Chopelas, 1991a; Chopelas, 1990, 1991). The most important modes are those below 450 cm^{-1}, as the estimates of heat capacity and entropy vs. temperature at ambient temperatures and below are very sensitive to the number of these modes and their distribution. These are, however, the most difficult to measure because of extensive overlapping, breadth of peaks and two-mode behavior in solid solutions, and low intensities in Raman spectra because of the low polarizabilities of the octahedral structural units.

The polarized Raman spectrum of forsterite has been previously described (Hohler and Funck, 1973; Servoin and Piriou, 1973; Iishi, 1978), but none of the results agree for the frequencies of the low intensity modes. The only other olivine for which a (nearly) complete single-crystal Raman spectrum has been described is tephroite (Mn_2SiO_4) (Stidham et al., 1976); partial data are available for Ca-bearing phases (e.g., Hohler and Funck, 1973; Piriou and McMillan, 1983). This study was prompted, in part, by the general lack of Raman data in the low frequency range for other olivines and, in part, by discrepancies with the previously reported data for forsterite (Chopelas, 1990).

In this study, single-crystal polarized Raman spectra of forsterite, olivine $(Mg_{0.88},Fe_{0.12})_2SiO_4$, monticellite, and fayalite are presented. Mode assignments to molecular motions are made by comparison of analogue modes in these olivines and previous results of tephroite (Stidham et al., 1976) and γ-Ca_2SiO_4 (Piriou and McMillan, 1983).

0003–004X/91/0708–1101$02.00

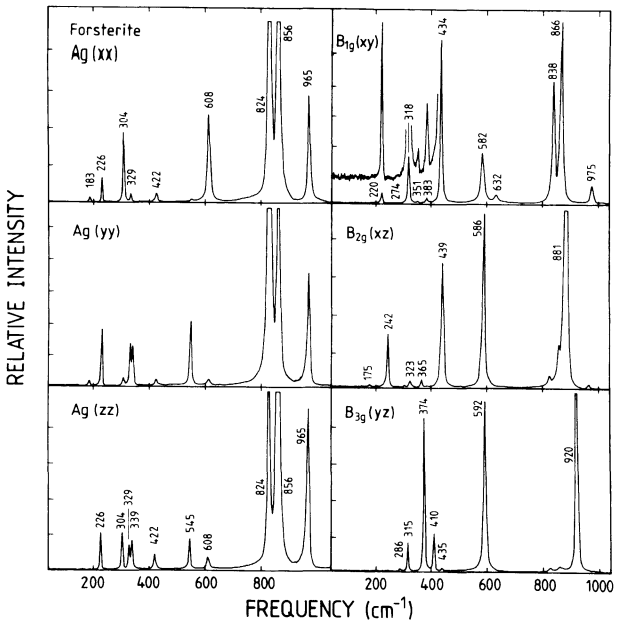

Fig. 1. Polarized Raman spectra of forsterite (Mg_2SiO_4). Polarizations and symmetries are indicated. Features not labeled in the B symmetries correspond to intensity leaked from other polarizations, allowed by the polarizing limit of the analyzer (0.9999). Polarization symbols do not represent sampling geometries as $(xz) = (zx)$, for example. The spectra are not smoothed or base line corrected.

The new spectral data are shown to be consistent with the single-crystal infrared results for forsterite and fayalite of Hofmeister (1987); the data also show that modes with the same assignments have similar mode Grüneisen parameters (Chopelas, 1990).

The thermodynamic parameters of olivines are calculated in a sequal paper (Chopelas and Hofmeister, in preparation) where the Raman and infrared data are combined to yield a complete set of vibrational frequencies for the above-mentioned olivines.

Experimental details

Synthetic end-member forsterite described by Suzuki et al. (1983), synthetic end-member and natural $(Fe_{0.94},Mn_{0.06})_2SiO_4$ fayalite described by Hofmeister (1987), and natural monticellite Ca $(Mg_{0.91},Fe_{0.09})SiO_4$ described by Sharp et al. (1986) were used. Single crystals of forsterite, monticellite, and synthetic fayalite were polished on the crystallographic faces, and the natural fayalite specimen was a thin (~10 μm) {100} cleavage plate. These were mounted on the optical bench, and final alignment of the crystals was made by observing the extinction of the A_g modes under crossed polarization (analyzer perpendicular to the laser polarization). These were not found to extinguish until the crystal was aligned to better than 0.5°. The spectra were either taken in a standard 90° Raman configuration or in a backscattering configuration, in which the laser light enters the sample at a 45° angle and the Raman spectrum is collected from the same face. The backscattering configuration did not change the relative intensities of the peaks.

The Raman spectra were excited by the 488.0-nm line of a Spectra Physics 2025-5 Ar ion laser, focused to 10 μm diameter in the sample. For the A_g modes of forsterite and the other olivines, powers of 20 to 200 mW sufficed to obtain the spectra. However, for the forsterite off-axis modes (B_{xg} modes, $x = 1$, 2, or 3), up to 1 W of power at the sample was required to bring the signal of the weakest modes above the minimal base line noise level. No shift or broadening of the Raman lines from the effects of heating was observed. An f = 2 lens collected the Raman signal and an f = 8 lens focused the image of the sample on the entrance port of the monochromator. The collection of the Raman signal over a large solid angle did not appear to mix the polarizations to a significant extent, as shown by the nearly complete extinctions of the modes in the other polarizations (see Figs. 1–3). Any spillover intensity from the other symmetries can be accounted for by the polarizing limit of the analyzing polarizer (0.9999). The Raman signal was analyzed with an ISA U1000 double monochromator equipped with a photon-counting detection system. The spectral resolution was 2 cm^{-1}, but

Table 1. Classification of the 81 optic modes of olivine by site group to factor group analysis

	$11A_g$	$11B_{1g}$	$7B_{2g}$	$7B_{3g}$	$10A_u$	$9B_{1u}$	$13B_{2u}$	$13B_{3u}$
SiO_4 internal	6	6	3	3	3	3	6	6
ν_1	1	1	0	0	0	0	1	1
ν_2	1	1	1	1	1	1	1	1
ν_3	2	2	1	1	1	1	2	2
ν_4	2	2	1	1	1	1	2	2
Lattice*	5	5	4	4	7	6	7	7
SiO_4 rot	1	1	2	2	2	2	1	1
SiO_4 trans	2	2	1	1	1	0	1	1
M1 trans	0	0	0	0	3	3	3	3
M2 trans	2	2	1	1	1	1	2	2
Activity**	R	R	R	R	0	ir	ir	ir

Note: From Farmer and Lazarev (1974); see Hofmeister (1987) for complete analysis.
* Abbreviations: rot = rotation; trans = translation.
** R = Raman active; 0 = not spectroscopically active; ir = infrared active.

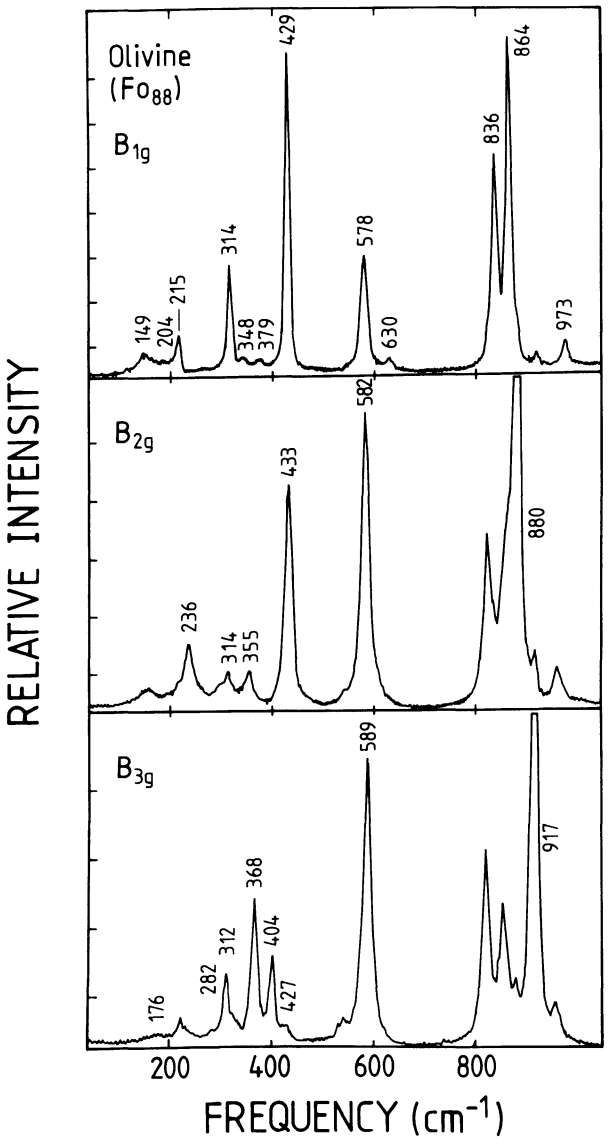

Fig. 2. Polarized Raman spectra of olivine $(Mg_{0.88},Fe_{0.12})_2SiO_4$ for the B symmetries obtained with the same spectrometer settings as for data in Figure 1 but with 10% of the laser power. These differ from data in Figure 1 by the significant broadening of the peaks, increased intensity under the base line, and the appearance of broad diffuse features below 220 cm^{-1}.

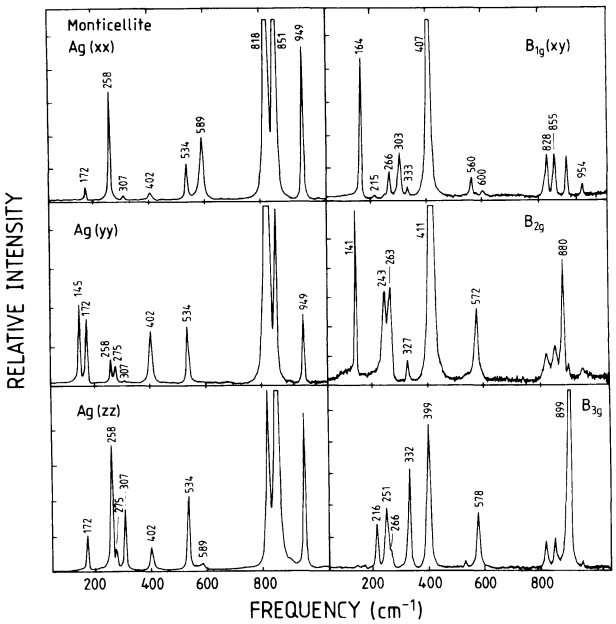

Fig. 3. Polarized Raman spectra of monticellite ($CaMgSiO_4$) analogous to those in Figure 1. These were obtained with the same spectrometer settings and laser power as those of olivine, Figure 2.

the spectra were sampled at 0.8 cm^{-1} (~0.2 Å) intervals. The range of frequencies for the spectra was 40 to 1040 cm^{-1}. All spectra were taken at 293 ± 1 K.

Spectroscopic results

Olivines are of orthorhombic (*Pbnm*) symmetry containing 4 M_2SiO_4 formula units per unit cell. Thus, olivines have 84 normal modes. By a symmetry analysis of the invariant atoms, the 84 vibrational modes belong to the irreducible representations of the point group D_{2h} (see, e.g., Hofmeister, 1987); the 81 optic modes are listed by symmetry in Table 1.

The olivine structure contains isolated SiO_4 units linked by octahedrally coordinated M^{2+} cations. The cations are in two crystallographically distinct sites, the smaller M1 (C_i symmetry) site and larger M2 (C_s symmetry) site. The M1 octahedron shares six edges with neighboring polyhedra, two with SiO_4 tetrahedra. The M2 octahedra share three edges with neighboring polyhedra but only one with an SiO_4 tetrahedron. From the greater extent of edge sharing between SiO_4 and $M1O_6$ polyhedra, one might expect that the M1 cation has a greater influence on the SiO_4 internal mode frequency. This does not appear to be the case (see the mode assignment section below).

By site group to factor group analysis (e.g., Farmer and Lazarev, 1974), one can determine the total number of modes of each motion type by assuming that the SiO_4 "molecules" retain their internal modes. This approximation is useful for determining frequency ranges for unobserved and inactive vibrational modes. In this analysis, shown in Table 1, no Raman active M^{2+} translations result from the M1 cation. The following sections describe new spectroscopic results listed in Table 2, correlated by analogous modes in each of the symmetries.

Forsterite

The Raman spectra of pure forsterite taken in six polarizations, presented in Figure 1, have well-formed peaks with a flat base line (no stray light, plasma lines, or fluorescence). The spectra as shown are not smoothed or

TABLE 2. Mode frequencies* in cm^{-1} of olivines and assignments

Fo_{100}	γ_i	Fo_{88}	Mo	Fa	Te	γ-Ca_2	Assignment
A_g							
965	0.66	961	949	932	935	925	ν_3
856	0.44	854	851	840	840	839	$\nu_1 + \nu_3$
824	0.48	822	818	814	808	814	$\nu_1 + \nu_3$
608	0.70	606	589	562	575		ν_4
545	0.53	542	534	505	515		ν_4
422	1.48	417	402	369	389		ν_2
339	1.87	334	275	237	256		M2 translation
329	1.16	326	307	289	291		SiO_4 rotation
304	1.63	301	258	259	244		M2 translation
226	0.67	222	172	171	167		SiO_4 translation
183	2.1	181	145	119	124		SiO_4 translation
B_{1g} (*xy*)							
975		973	954	947	—		ν_3
866		864	855	851	—	849	$\nu_3 (+ \nu_1)$
838		836	828	822	820		$\nu_1 (+ \nu_3)$
632		630	600	577	588		ν_4
582	0.66	578	560	524	546		ν_4
434	1.4	429	407	384	393		ν_2
383		379	333	312	307		M2 translation
351		348	303	277?	288		M2 translation
318		314	266	260	271		SiO_4 rotation
274		—	215	193	203		SiO_4 translation
220		215	164	154	155		SiO_4 translation
B_{2g} (*xz*)							
881	0.44	880	879	860	—		ν_3
586		582	572	553	553		ν_4
439	1.6	433	411	405	401		ν_2
365		355	327	309	319		mix (SiO_4 rot)
323		314	263	290	274		mix (M2 trans)
242	1.21	236	243	189	188		mix (SiO_4 rot)
175		—	141	102	119		mix (SiO_4 trans)
B_{3g} (*yz*)							
920	0.38	917	899	900	892	887	ν_3
592		589	578	549	555		ν_4
435		427	332	—	304		mix (SiO_4 rot)
410	0.99	404	399	376	378		ν_2
374	1.75	368	266	281	276		mix (M2 trans)
315		312	251	186	223		mix (SiO_4 rot)
286		282	216	113	137		mix (SiO_4 trans)
43.65			51.56	46.15	48.61	59.11	V_0^{298} (cm^3 mol^{-1})**
0.203		0.189	0.176	0.134	0.135	0.158	$1/\sqrt{M}$

Note: Fo = forsterite, this study; γ_i = mode Grüneisen parameter from Chopelas (1990a); Fo_{88} = $(Mg_{88},Fe_{12})_2SiO_4$, this study; Mo = monticellite, this study; Fa = fayalite, this study; Te = tephroite, taken at 14 K by Stidham et al. (1976); α-Ca_2 = α-Ca_2SiO_4, Piriou and McMillan (1983); M = average of M^{2+} masses (see Fig. 6).

* The uncertainties for the frequencies of this work are 1 cm^{-1}.

** Quoted from Sharp et al. (1986).

base line corrected. The other three off-axis polarizations yielded identical results to those shown and are not presented; thus, $(xy) = (yx)$. On the other hand, the Raman spectra of mantle-relevant olivine (Fo_{88},Fa_{12}) have broader peaks and uneven base lines, especially below 500 cm^{-1}, shown in Figure 2 for the B_{xg} (x = 1, 2, or 3) modes. Additional broad features appeared in the spectra of Fo_{88} below 200 cm^{-1} that do not appear to be fundamental Raman modes or related to two-mode behavior (where two modes appear in intermediate compositions, the intensity of each reflecting the relative proportions of the cations). Similar features were found in the Raman of pyrope (Mg_{94}) (Hofmeister and Chopelas, 1991b) at low frequencies and may represent some forbidden lattice modes appearing because of the reduction of symmetry by the substitution of other elements in the cation sites. The frequency shift from the substitution of 12% Fe for the Mg is used to help determine mode assignments in a following section, while keeping in mind that any two-mode behavior would not lead to proportional shifts for some of the modes. All but the two weakest fundamental modes were found in the olivine (Fo_{88}).

Although the forsterite spectra in Figure 1 appear to be similar in relative intensity for the higher intensity modes to those previously published (e.g., Iishi, 1978; Hohler and Funck, 1973), the lowest intensity modes in the three B_{xg} symmetries differ from those of any previous work. In B_{1g}, clear modes were found at 352 cm^{-1} and 383 cm^{-1}, and a weak mode was found at 274 cm^{-1} instead of modes at 165, 192, 260, and 418 cm^{-1} as found by Iishi (1978) or Servoin and Piriou (1973). Of all 36 Raman modes in the spectrum, only the 274 cm^{-1} mode had less than a 3:1 signal to noise ratio. This value is supported as a fundamental mode by the appearance of a low-intensity analogue B_{1g} mode in monticellite (next section) and tephroite (Stidham et al., 1976). In B_{2g}, a weak but clear

mode was found at 175 cm^{-1} instead of 142 cm^{-1} as reported by Iishi (1978). In B_{3g}, clear modes were found at 286 and 435 cm^{-1} instead of those reported at 226 and 272 cm^{-1} by Iishi (1978). The source of the previously reported modes may have been incomplete extinction of modes in other polarizations or impurity effects (mentioned above), as suggested by a comparison of the peak widths and base lines of the spectra of Iishi (1978) with those in Figure 1. These new modes were confirmed by several repeat spectra in different configurations, i.e., those for both (xy) and (yx) configurations for B_{1g}, and those with a slight rotation of the crystal that caused relative intensity changes among the modes.

The new modes are supported by analogous modes in the other olivines and the similarity of the forsterite single-crystal infrared results of Hofmeister (1987), where only two modes were found below 268 cm^{-1}. This is consistent with the number of modes expected for this frequency range by factor group analysis (see the mode assignment section below). The results of this study decrease the number of modes below this value from eight to five in the Raman spectrum. This may seem trivial at first, but the calculation of the heat capacity and entropy is very sensitive to the number of modes below 300 cm^{-1} (Chopelas and Hofmeister, in preparation).

Thirty-three of the 36 mode frequencies in Table 2 are also accurately predicted by lattice dynamical calculations that did not use the spectral data to tune the input parameters (Price et al., 1987a, 1987b). The only discrepant values are the three lowest frequency modes in B_{3g}. For these modes, the trends of frequency vs. composition suggest extensive mode mixing for this polarization (see the mode assignment section below).

Monticellite

The crystal quality and purity of the natural monticellite was sufficient to produce sharp, well-formed peaks even in the low energy range (Fig. 3). The small amount of Fe present in this sample is not expected to affect significantly the results, as (1) the high-energy modes are in agreement with those of a pure synthetic monticellite sample (Piriou and McMillan, 1983) and (2) Ca^{2+} occupies essentially all the M2 sites and the M1 translations are not Raman active. The greater intensity of the low energy analogue modes compared with forsterite reflects the increased polarizability of the CaO_6 structural units. The same effect was found for the Ca garnets (Hofmeister and Chopelas, 1991b). Caution must be used in determining analogous modes for the olivines because the relative intensities vary with composition.

All of the modes predicted by symmetry in each of the polarizations were easily found and are listed in Table 2 with their forsterite counterparts. The high-energy modes are in agreement with previous powder Raman data (Piriou and McMillan, 1983). Notice that polarized single-crystal studies are required to resolve and assign the six modes between 534 and 600 cm^{-1} and four modes between 399 and 411 cm^{-1} shown as broad bands in the powder data of Piriou and McMillan (1983). This also occurs for tephroite (Stidham et al., 1976) and fayalite (see below).

The three A_g polarizations help correlate the monticellite modes to those of forsterite. In $A_g(xx)$ in forsterite, the 304 cm^{-1} mode is very intense and the 339 cm^{-1} mode disappears; in $A_g(yy)$, the opposite is true. The analogous behavior in monticellite results in a correlation of the 258, 307, and 276 cm^{-1} modes in monticellite with the 304, 329, and 339 cm^{-1} modes in forsterite, respectively. A similar correlation of the modes might occur in B_{1g} since this symmetry represents modes that have split due to lowering of symmetry (Davydov splitting). For the remaining two symmetries, analogous modes in the two minerals were assumed to appear consecutively as a first approximation.

Fayalite

Laser powers in excess of 20 mW caused heating or melting of the dark synthetic fayalite. This resulted in spectra with lower signal-to-noise ratios, especially for the B_{xg} modes (see Fig. 4). The laser power limitation also prevented the resolution of the seventh B_{3g} mode and the eleventh B_{1g} mode. A feature at 277 cm^{-1}, appearing in several repeat spectra of B_{1g}, may be the missing mode in this configuration, but it was not as clearly resolvable as the other peaks.

There are two high-energy broad features in A_g symmetry that are not fundamental modes, as they are much broader than the other modes and have no analogy in the other olivines. In addition, the intermediate modes at 365–405 cm^{-1} and 505–580 cm^{-1} are broader than their counterparts in the other olivines. These effects have also been observed for the Raman spectra of almandine (Hofmeister and Chopelas, 1991b). It has been shown recently that the intermediate modes become significantly narrower at lower temperatures, an effect ascribed to anharmonicity (Sharma and Cooney, 1990). The broad, high-energy features appear to be related to the Fe^{3+} content of the fayalite (S. K. Sharma, personal communication, 1990).

The natural fayalite $(Fe_{0.94},Mn_{0.06})_2SiO_4$ sample was a 10-μm thick × 30-μm × 30-μm {100} cleavage plate. Only unpolarized spectra aligned along the y and z axes were obtained; Figure 5 shows the $A_g(yy)$ or $A_g(zz) + B_{3g}$ polarizations. Some of the other modes in B_{2g} and B_{3g} were also shown as either shoulders on the high energy modes or weak modes in the low-frequency ranges by spectra taken as the sample was rotated about the collection (crystal's X) axis. The results, shown in Figure 5, show that the observed mode frequencies for the natural fayalite are very similar to those observed for the synthetic fayalite, as would be expected by the similarity in mass and cation radii of Mn^{2+} and Fe^{2+}. The peaks in the natural sample are also broader, as observed for the natural olivine Fo_{88} in this study.

For three high-energy Raman modes in Fe-Mg solid solutions, i.e., modes at 920, 856, and 824 cm^{-1} in for-

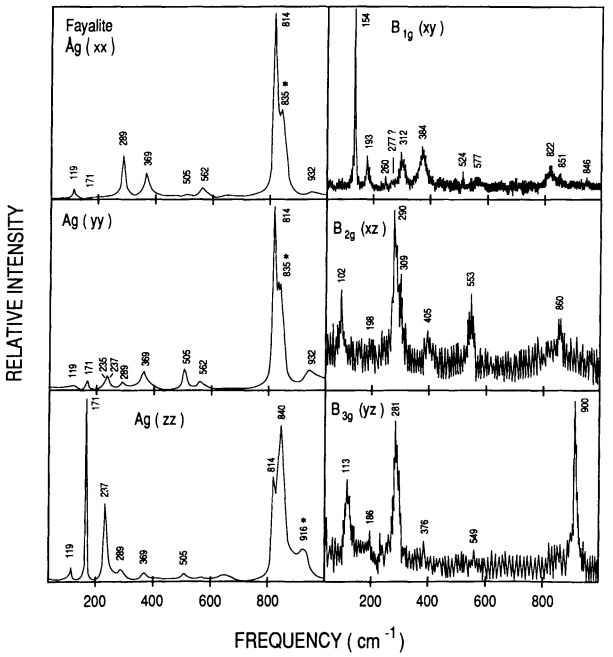

Fig. 4. Polarized Raman spectra of synthetic fayalite (Fe_2SiO_4) analogous to those in Figure 1. These were obtained with the same spectrometer settings as those of olivine, Figure 2, but laser power was limited to 20 mW at the dark sample. Broad, high energy features marked with an asterisk (*) are not fundamental modes.

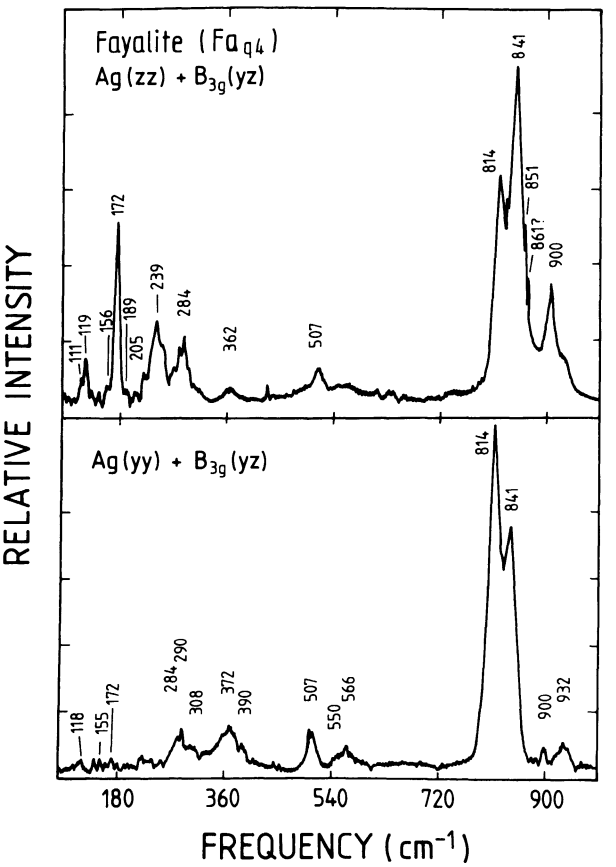

Fig. 5. Unpolarized Raman spectra of fayalite $(Fe_{0.94}Mn_{0.06})_2SiO_4$ obtained from a {100} cleavage plate. Modes other than those in A_g and B_{3g} were found by rotating the crystal about the collection (X axis of the crystal). The spectra pictured represent a composite of 18 different spectra taken in different orientations.

sterite, it has been shown that the frequency varies linearly with Fe content to 80% Fe (Guyot et al., 1986). The results for fayalite (Table 2) lie at the extrapolated values for 100% Fe. Powder infrared data also show that the SiO_4 internal modes also vary linearly with composition within a solid solution (Burns and Huggins, 1972), so it is expected that the values for Fo_{88} in Table 2 should lie intermediate to those for forsterite and fayalite. Discounting modes with two-mode behavior, this appears to be the case (see next section).

Mode assignments

The frequency changes due to cation substitution are fundamental to understanding changes in certain macroscopic physical properties such as heat capacity, entropy, and compressibility. The first step to understanding the connection between vibrational spectra and these physical properties is the assignment of the modes to atomic motions. In this case, this is done by cross comparison of the analogous modes for the various olivine species. Cation substitution for Mg^{2+} in forsterite serves to cause a decrease in mode frequencies, mainly because of increased mass or increased volume. Other effects might include coupling and mode mixing.

In addition to the present measurements for forsterite, monticellite, and fayalite, the single-crystal Raman study of tephroite by Stidham et al. (1976) is complete in the low-frequency range. Their results are interpreted using the results of this study and listed in Table 2. The effects of cation mass and volume on the mode frequencies are distinguished by comparing the effect of the largest cation (Ca^{2+}) vs. the heaviest (Fe^{2+}) on the mode frequencies.

The mode Grüneisen parameter, γ_i, derived from the pressure shift of the modes should also correlate very closely, because the volume change during compression is caused by compression of the voids and MO_6 octahedra but not the SiO_4 tetrahedra. Therefore, it is expected that the lattice modes would have higher γ_i values than the SiO_4 internal modes, as appears to be the case (see Table 2). Exceptions are discussed below.

SiO_4 internal modes

In the factor group method (e.g., Farmer and Lazarev, 1974), the four internal SiO_4 frequencies are assumed to be retained in the spectra but slightly modified by the crystal environment, e.g., symmetry of the site and nearest neighbor distances. This is a viable approximation when the SiO_4 internal mode frequencies are significantly

higher than the lattice modes, as appears to be the case for olivines.

The symmetric stretching frequency ν_1 should vary the least with changing composition. However, the two intense high-energy A_g modes vary by about the same small amount for the range of compositions. This is consistent with the suggestion that these modes contain both ν_1 and asymmetric stretching ν_3 character (Paques-Ledent and Tarte, 1973; Piriou and McMillan, 1983). In B_{1g}, the two intense high-energy modes vary more with composition than do the corresponding A_g modes but the fact that they both vary by the same amount suggests the same type of mode mixing. The remaining high-energy modes are assigned ν_3 and are in accord with the number and symmetry expected from the symmetry analysis.

The frequency variation of the high-energy modes for the olivines (data given in Table 2) is quite small but is obviously affected by the cation substitution. A plot of frequency vs. $1/\sqrt{M}$, where M represents the average of the two cation masses, shows that most of the modes vary linearly with this parameter (see Fig. 6). This parameter represents the frequency change of an oscillator, resulting from a change in mass, from $\nu \propto \sqrt{k/m}$, where ν is the frequency of an oscillator, k the force constant, and m the mass. There have been extensive discussions of whether the two intense A_g high-energy mode frequencies depend on the volume of the M1 site (Piriou and McMillan, 1983) or on O-O distances that are distorted from ideal symmetry (Lam et al., 1990) in response to Ca^{2+} substitution in the M sites. If tephroite or fayalite are included in this analysis, the heavier but relatively small cations cause a decrease in the mode frequencies by an even larger amount. However, it is clear from Figure 6 that all modes do not fall on linear trends, e.g., those at 965 and 920 cm^{-1} in forsterite, indicating some dependence of frequency on something else, such as cation volume or coupling effects.

If the SiO_4 bending modes are assigned to the next highest frequencies (except for the 435 B_{3g} mode in forsterite), the number and symmetry of the bending modes for all four symmetries agree with those predicted by symmetry analysis. The 435 cm^{-1} B_{3g} mode in forsterite did not fall on the trends for data from the other olivines; it was of much weaker intensity, and it shifted by a larger amount than the other bending modes by substitution of 12% Fe for Mg and thus was assigned to a lattice mode. Even though the bending modes are very similar in frequency for all of the symmetries, they generally occur in the same frequency order for the olivines for which data are reported in Table 2; that is, none of the lines shown in Figure 6 crosses another. The same general small shifts as a function of composition found for the SiO_4 stretching modes were found for the bending modes, except that the monticellite ν_2 modes were below the lines connecting data points for the other olivines, indicating either some dependence of these on volume or mixing with other modes. The latter is more likely because the mode Grüneisen parameters for these modes in forsterite are sig-

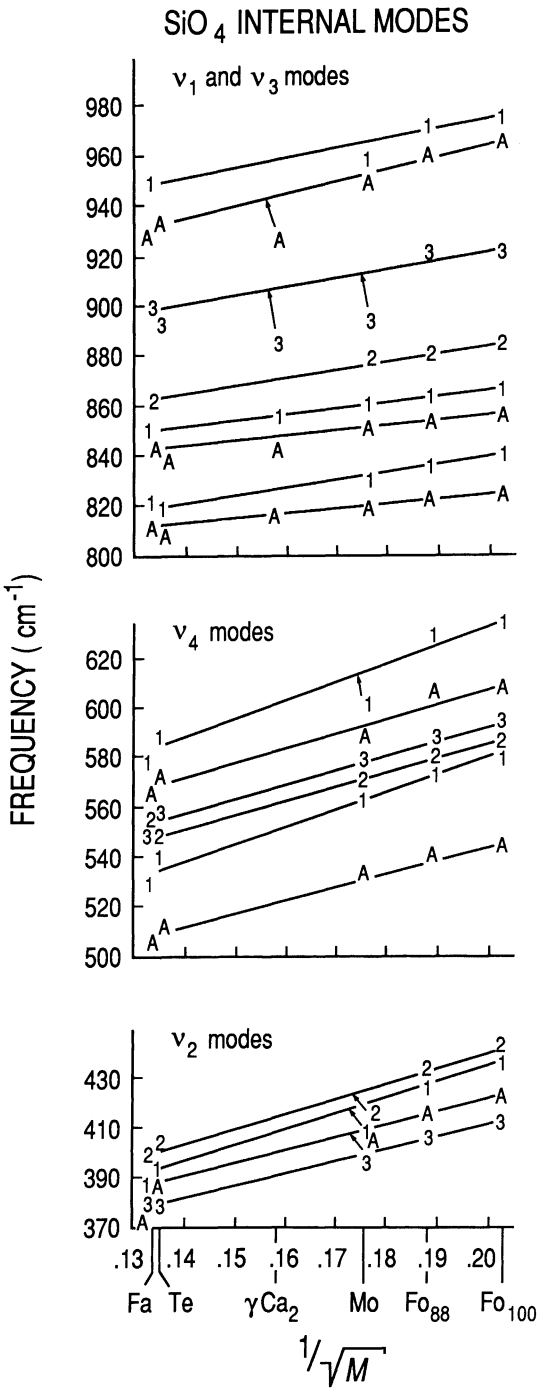

Fig. 6. Plots of the SiO_4 internal modes vs. the parameter $1/\sqrt{M}$ (listed in Table 2 for the various olivines), representing the change in vibrational frequency with mass. M is the average of the cation masses; for example, for monticellite $M = (24.3 + 40.1)/2$. The symbols represent the symmetries of the observed modes as follows: A = A_g; 1 = B_{1g}; 2 = B_{2g}; 3 = B_{3g}; minerals: Fa = fayalite; Te = tephroite; γCa_2 = γ-Ca_2SiO_4; Mo = monticellite; Fo_{88} = $(Mg_{0.88},Fe_{0.12})_2SiO_4$; Fo_{100} = forsterite.

nificantly greater than for the other internal modes. The extent of the mixing might be resolved by studies of solid solutions.

Lattice modes

The variation of the remaining lattice modes with composition is much larger than for the SiO_4 internal modes. Among the lattice modes, the SiO_4 rotations are expected to have the highest frequency and vary the least; the SiO_4 translations, to be the lowest in frequency; and the SiO_4 and M2 translations to be mixed, as observed for the orthosilicate, garnet (Hofmeister and Chopelas, 1991b). These appear to be the case for the olivines. For the A_g modes of forsterite and monticellite, the 329 cm^{-1} forsterite mode correlated with the 307 cm^{-1} monticellite mode and the 291 cm^{-1} tephroite mode. Since it varied the least among the lattice modes, this was assigned to an SiO_4 rotation (see discussion on rotational modes in Hofmeister and Chopelas, 1991b). The 339 and 304 cm^{-1} modes in forsterite were then assigned to M2 translations; they are in agreement with the number predicted by symmetry analysis and have the highest mode Grüneisen parameters in this range. The remaining 183 and 226 cm^{-1} modes in forsterite were assigned SiO_4 translations. Similar trends were found for B_{1g} and were likewise assigned. The mode Grüneisen parameter for the 183 cm^{-1} forsterite mode is consistent with those observed for other silicates (diopside, enstatite, Chopelas, in preparation; β-Mg_2SiO_4, Chopelas, 1991).

It is not expected or observed that the mode frequencies measured for Fo_{88} lie proportionately between those for fayalite and forsterite. Observations of two-mode behavior of the cation translations for pyrope-almandine solid solutions (Hofmeister and Chopelas, 1991b) indicate this might occur for the forsterite-fayalite solid solution series as well. Recall that two-mode behavior occurs when two modes, one representing each end-member, appear in the spectrum of a binary solid solution. The frequencies of these modes are nearly the same as those observed for each end-member, and the intensities of the two modes represent the relative proportions of each cation present. Thus, those lattice modes showing the least frequency shift may be part of two-mode behavior for the cation translations; the Fe counterpart in the spectrum is probably too weak to be seen because of the low Fe content of the olivine. This appears to be nearly the case in A_g, especially considering that the Fe^{2+} preferentially substitutes at the large M2 site and a proportionate shift of the M2 cation translations should be about 10 to 15 cm^{-1}, which is clearly not observed.

The B_{2g} and B_{3g} lattice modes appear to be mixed to varying degrees in the olivines since from forsterite to fayalite the frequency changes from 50 to 75 cm^{-1} in B_{2g} and from 110 to 175 cm^{-1} in B_{3g}. In addition, the monticellite modes are not intermediate in frequency, suggesting a strong dependence on volume or other effects for these modes. Interpretation of the spectra would require Raman spectra of olivines of intermediate compositions and a single crystal study of γ-Ca_2SiO_4 to define the frequency trends and reveal any two-mode behavior. These are interpreted as mixed modes but are estimated to have the largest contribution (noted in brackets in Table 2) by comparison with modes in other symmetries, in the absence of further experiments that could better explain the observations.

In comparing the frequencies of the various mode categories, the frequency ranges for forsterite and fayalite found in this study are seen to be similar to those found for the infrared spectra of Hofmeister (1987). These are also the frequency ranges that lead to the best match of the calculated heat capacity and entropy with calorimetric data (see Hofmeister, 1987; Chopelas, 1990), suggesting that not only can accurate spectral data yield good estimates of thermodynamic properties but the opposite may also be true: that accurate thermodynamic properties can be used to estimate spectral properties. More details regarding the thermodynamics of olivines will be presented in a subsequent paper (Chopelas and Hofmeister, in preparation).

Acknowledgments

I thank A.M. Hofmeister for valuable discussions and contribution of the monticellite and natural fayalite samples for this study; R.J. Hemley for contributing the synthetic fayalite; and Ph. Gillet, R. Boehler, and an anonymous reviewer for helpful comments on the manuscript.

References cited

Burns, R.G., and Huggins, F.E. (1972) Cation determinative curves for Mg-Fe-Mn olivines from vibrational spectra. American Mineralogist, 57, 967–985.

Chopelas, A. (1990) Thermal properties of forsterite at mantle pressures derived from vibrational spectroscopy. Physics and Chemistry of Minerals, 17, 149–156.

——— (1991) Thermal properties of β-Mg_2SiO_4 at mantle pressures derived from vibrational spectroscopy: Implications for the mantle at 400 km depth. Journal of Geophysical Research, in press.

Farmer, V.C., and Lazarev, A.N. (1974) Symmetry and crystal vibrations. In V.C. Farmer, Ed., The infrared spectra of minerals, p. 51–68. Mineralogical Society, London.

Guyot, F., Boyer, H., Madon, M., Velde, B., and Poirier, J.P. (1986) Comparison of the Raman microprobe spectra of $(Mg,Fe)_2SiO_4$ and Mg_2SiO_4 with olivine and spinel structure. Physics and Chemistry of Minerals, 13, 91–95.

Hofmeister, A.M. (1987) Single-crystal absorption and reflection infrared spectroscopy of forsterite and fayalite. Physics and Chemistry of Minerals, 14, 499–513.

Hofmeister, A.M., and Chopelas, A. (1991a) Thermodynamic properties of pyrope and grossular from vibrational spectroscopy. American Mineralogist, 76, 880–891.

——— (1991b) Vibrational spectroscopy of end-member silicate garnets. Physics and Chemistry of Minerals, 17, 503–526.

Hofmeister, A.M., Xu, J., Mao, H.-K., Bell, P.M., and Hoering, T.C. (1989) Thermodynamics of Fe-Mg olivines at mantle pressures: Mid- and far-infrared spectroscopy at high pressure. American Mineralogist, 74, 281–306.

Hohler, V., and Funck, E. (1973) Schwingungsspektren im Kristallen mit Olivin-Struktur I. Silikate. Zeitschrift für Naturforschung, 28B, 125–139 (in German).

Iishi, K. (1978) Lattice dynamics of forsterite. American Mineralogist, 63, 1198–1208.

Kieffer, S.W. (1979) Thermodynamics and lattice vibrations of minerals: 3 Lattice dynamics and an approximation for minerals with application

to simple substances and framework silicates. Reviews of Geophysics and Space Physics, 17, 35–59.

Kovach, J.J., Hiser, A.L., and Karr, C., Jr. (1975) Far infrared spectroscopy of minerals. In C. Karr, Jr., Ed., Infrared and Raman spectra of lunar and terrestrial minerals. Academic Press, New York.

Lam, P.K., Yu, R., Lee, M.W., and Sharma, S.K. (1990) Structural distortions and vibrational modes in Mg_2SiO_4, American Mineralogist, 75, 109–119.

Paques-Ledent, M.T., and Tarte, P. (1973) Vibrational studies of olivine type compounds I. The i.r. and Raman spectra of the isotopic species of Mg_2SiO_4. Spectrochimica Acta, 29A, 1007–1016.

Piriou, B., and McMillan, P. (1983) The high frequency vibrational spectra of vitreous and crystalline orthosilicates. American Mineralogist, 68, 426–443.

Price, G.D., Parker, S.C., and Leslie, M. (1987a) The lattice dynamics of forsterite. Mineralogical Magazine, 51, 157–170.

——— (1987b) The lattice dynamics and thermodynamics of the Mg_2SiO_4 polymorphs. Physics and Chemistry of Minerals, 15, 181–190.

Rao, K.R., Chaplot, S.L., Chowdhury, N., Ghose, S., Hastings, J.M., and Corliss, L.M. (1988) Lattice dynamics and inelastic neutron scattering from forsterite, Mg_2SiO_4: Phonon dispersion relation, density of states, and specific heat. Physics and Chemistry of Minerals, 16, 83–97.

Servoin, J.L., and Piriou, B. (1973) Infrared reflectivity and Raman scattering of Mg_2SiO_4 single crystal. Physica Status Solidi, B55, 677–686.

Sharma, S.K., and Cooney, T.F. (1990) Raman spectral study of Fe_2SiO_4, Mg_2SiO_4, Mn_2SiO_4, and Ni_2SiO_4 olivines between 15 and 293 K. Eos, 71, 525.

Sharp, Z.D., Essene, E.J., Anovitz, L.M., Metz, G.W., Westrum, E.F., Jr., Hemingway, B.S., and Valley, J.W. (1986) The heat capacity of natural monticellite and phase equilibria in the system CaO-MgO-SiO_2-CO_2. Geochimica et Cosmochimica Acta, 50, 1475–1484.

Stidham, H.D., Bates, J.B., and Finch, C.B. (1976) Vibrational spectra of synthetic single crystal tephroite, Mn_2SiO_4. Journal of Physical Chemistry, 80, 1226–1234.

Suzuki, I., Anderson, O.L., and Sumino, Y. (1983) Elastic properties of single crystal forsterite Mg_2SiO_4, up to 1,200 K. Physics and Chemistry of Minerals, 18, 38–46.

Tarte, P. (1963) Etude infra-rouge des orthosilicates et des orthogermanates structure du type olivine et monticellite. Spectrochimica Acta, 19, 25–47 (in French).

Manuscript received May 29, 1990
Manuscript accepted April 9, 1991